Triaxial quadrupole dynamics and the inner fission barrier of some heavy even-even nuclei

K. Benrabia and D. E. Medjadi
Laboratoire N-corps et Structure de la Matière, Ecole Normale Supérieure, BP 92, Vieux Kouba, 16050 Alger, Algéria

M. Imadalou
Laboratoire N-corps et Structure de la Matière, Ecole Normale Supérieure, BP 92, Vieux Kouba, 16050 Alger, Algéria and Faculté des Sciences, Département de Physique, Université Saad Dahlab de Blida, Route de Soumâa, BP 270 Blida, Algéria

P. Quentin*
Division of Nuclear Physics, Ton Duc Thang University, Ho Chi Minh City, Vietnam; Faculty of Applied Sciences, Ton Duc Thang University, Ho Chi Minh City, Vietnam; Université de Bordeaux, CENBG, UMR5797, F-33170 Gradignan, France; and CNRS, IN2P3, CENBG, UMR5797, F-33170 Gradignan, France

(Received 5 May 2017; revised manuscript received 13 June 2017; published 21 September 2017)

Background: Inner fission barriers of actinide nuclei have been known for a long time to be unstable with respect to the axial symmetry. On the other hand, taking into account the effect of the relevant adiabatic mass parameter reduces or even may wash out this instability. A proper treatment of the dynamics for both axial and triaxial modes is thus crucial to accurately determine the corresponding fission barriers. This entails in particular an accurate description of pairing correlations.

Purpose: We evaluate the potential energies, moments of inertia, and vibrational mass parameters in a two-dimensional relevant deformation space (corresponding to the usual β and γ quadrupole deformation parameters) for four actinide nuclei (^{236}U, ^{240}Pu, ^{248}Cm, and ^{252}Cf). We assess the relevance of our approach to describe the dynamics for a triaxial mode by computing the low energy spectra (exploring thus mainly the equilibrium deformation region). We evaluate the inner fission barrier heights releasing the axial symmetry constraint.

Method: Calculations within the Hartree-Fock plus BCS approach are performed using the SkM* Skyrme effective interaction in the particle-hole channel and a seniority force in the particle-particle channel. The intensity of this residual interaction has been fixed to allow a good reproduction of some odd-even mass differences in the actinide region. Adiabatic mass parameters for the rotational and vibrational modes are calculated using the Inglis-Belyaev formula supplemented by a global renormalization factor taking into account the so-called Thouless-Valatin corrections. Spectra are obtained through the diagonalization of the corresponding Bohr collective Hamiltonian.

Results: The experimental low energy spectra are qualitatively well reproduced by our calculations for the considered nuclei. Inner fission barrier heights are calculated and compared with available estimates from various experimental data. The reproduction of the data is better for ^{236}U and ^{240}Pu (up to about 300 keV) than for ^{248}Cm and ^{252}Cf (up to about one MeV).

Conclusions: While these results are encouraging, they call for, in particular, a better treatment of pairing correlations, especially as far as the particle number conservation is concerned. Besides, these results could provide a basis for the determination of the least action trajectories which would generate better grounds for the evaluation of fission half lives.

DOI: 10.1103/PhysRevC.96.034320

I. INTRODUCTION

It has long been known [1] that static calculations yield solutions around the inner fission saddle point which break the axial symmetry. However, in approaches determining the least action trajectory in the classical mechanical sense, it has appeared that a tendency towards a restoration of the axial symmetry could be found. This was first advocated in calculations of fission barriers for some superheavy nuclei [2]. Recently, the same trend has been found in more elaborate approaches including pairing correlations as collective modes for ^{240}Pu in Ref. [3] and for ^{250,264}Fm in Ref. [4]. Nevertheless, it is clear that such results are strongly contingent upon a correct static description of the potential energy surface (PES) as well as of a relevant assessment of the collective kinetic energy parameters along and around the preferred trajectory. It seems therefore relevant to check, as a useful starting point for microscopic evaluations of fission barrier heights, to what extent they are able to reasonably describe the dynamics associated with the triaxial degree of freedom. This will be assessed in what follows by evaluating the low energy spectroscopy for the full (five-dimensional) quadrupole modes in the ground state well, within the same framework as the one used to determine the potential energy surface (PES) in the vicinity of the inner fission saddle point.

*Corresponding author: philippe.quentin@tdt.edu.vn

Moreover, as is well known, PES results, hence in particular fission barrier heights, may be considered even in purely microscopic approaches to depend ultimately on two underlying ingredients: bulk (liquid drop or semiclassical) properties associated to the effective interaction in use and the averaged single-particle level densities at the Fermi surface $\tilde{g}(\lambda)$ which are produced within a mean-field approach. For the former ingredient, let us recall that the SkM* parametrization of the Skyrme interaction [5] has been used here. Indeed, it has been explicitly fitted from its original SkM version [6] to reproduce supposedly good liquid drop barriers. The second factor impacting the reproduction of the experimental barriers is strongly associated with the quality of calculated pairing correlations. Obtaining them adequately reflects good level density properties and has a very important effect on relative energies, particularly on fission barrier heights. It is clear (as exhibited from the first Strutinsky's type calculations) that shell effects are partially damped by pair correlations. Increasing these correlations acts in opposite directions near local minima and around local extrema. As a result it diminishes fission barrier heights. In this context, we emphasize that the intensities of the residual interaction in use here were carefully determined in Ref. [7] so as to reproduce reasonably well data on odd-even mass differences (taken here from Ref. [8]) in the considered region of the nuclear chart. This prescription is allegedly the usual procedure to parametrize it or, at least, doing so is generally advocated. But, in practice, it is implemented merely through a fit of lowest quasiparticle energies. In our case, such a reproduction has been demonstrated, at least roughly, from explicit mass calculations for both even-even and even-odd neighboring nuclei within Hartree-Fock plus BCS calculations with self-consistent blocking in the latter case.

More specifically, PESs have been evaluated through self-consistent Hartree-Fock plus BCS calculations under two constraints: on the intrinsic values of the Q_{20} and Q_{22} usual quadrupole moments. While the SkM* Skyrme interaction has been used as already mentioned for the particle-hole channel, a seniority interaction has been considered to solve the gap equations. The three moments of inertia and the three vibrational mass parameters have been evaluated within the Inglis-Belyaev [9] approximation of the adiabatic time-dependent Hartree-Fock-Bogoliubov (ATDHFB) approach (see [10] and [11]) supplemented by a rough estimate of the momentum operator [11] as well as of the missing self-consistent terms dubbed Thouless-Valatin [12] corrections. The latter have been taken care of as in Ref. [13] (see the extended discussion of Sec. II B). This has provided us with a microscopically determined quadrupole Bohr Hamiltonian [14] valid in particular for the ground state well, thus yielding eigensolutions describing the low energy quadrupole dynamics of the nuclei under consideration.

This paper will be organized as follows. In Sec. II, the formalism in use will be briefly sketched together with some relevant calculational details and approximations. Section III will be devoted to the presentation and discussion of the obtained results for the ground state well and the inner fission barrier region. Finally, some conclusions and directions for further studies will be detailed in Sec. IV.

II. THEORETICAL FRAMEWORK, APPROXIMATIONS, AND SOME CALCULATIONAL DETAILS

A. Solving the constrained Hartree-Fock plus BCS equations

The essentials of the solution of the constrained Hartree-Fock plus BCS (HF + BCS) equations, as performed here, were described at length a long time ago for axially symmetric solutions in Ref. [15] and in Ref. [16] whenever axial symmetry is broken. In both references, the codes in use preserve the intrinsic parity symmetry.

Calculations are performed under constraints on the quadrupole moments corresponding to the two operators $\widehat{Q}_{02}$ and $\widehat{Q}_{22}$ given by

$$\widehat{Q}_{20} = 2\hat{z}^2 - \hat{x}^2 - \hat{y}^2, \quad \widehat{Q}_{22} = \hat{y}^2 - \hat{x}^2. \tag{1}$$

From the corresponding expectation values, one deduces, as usual, some β and γ quadrupole shape parameters defined as

$$\beta = \frac{\pi}{5}\frac{\sqrt{\langle\widehat{Q}_{20}\rangle^2 + 3\langle\widehat{Q}_{22}\rangle^2}}{A\langle\hat{r}^2\rangle}, \quad \tan\gamma = \frac{\sqrt{3}\langle\widehat{Q}_{22}\rangle}{\langle\widehat{Q}_{20}\rangle} \tag{2}$$

involving the expectation value of the $\hat{r}^2$, $\widehat{Q}_{02}$, and $\widehat{Q}_{22}$ operators and where A is the total number of nucleons. As is well known, in the (β,γ) plane the radial coordinate β is an A-independent measure of the global quadrupole deformation while the angle γ determines the triaxiality of the nuclear distribution.

The expansion of canonical basis states on axially symmetric harmonic oscillator states can be made, in a first stage, in the coordinate representation in terms of normalized Hermite and associated Laguerre polynomials $H_{n_z}(\xi)$ and $L_{n_r}^{|\Lambda|}(\eta)$ (see [17]) as

$$\varphi_\mu(r,\theta,z) = \sqrt{\frac{\beta_z\beta_\perp^2}{pi}}e^{-(\xi^2+\eta)/2}e^{i\Lambda\theta}\eta^{|\Lambda/2|}H_{n_z}(\xi)L_{n_r}^{|\Lambda|}(\eta), \tag{3}$$

where μ represents the set (n_r,n_z,Λ) of the harmonic oscillator basis quantum numbers, while β_z and $\beta_\perp$ are the usual oscillator constants, and finally ξ and η are given in terms of the cylindrical coordinates r and z by $\xi = z\beta_z$ $\eta = r^2\beta_\perp^2$.

Then, the above states are combined to provide a basis where both the x signature and the intrinsic parity are conserved quantum numbers (see Ref. [16]), so that

$$|\mu,s\rangle = \frac{\sqrt{2}}{2}(\phi_\mu\chi_{1/2} + s(-1)^{n_z}\phi_{\overline{\mu}}\chi_{-1/2}), \quad s = \pm 1. \tag{4}$$

Here we have introduced $\overline{\mu} = (n_r,n_z,-\Lambda)$ and $\chi_{\pm\frac{1}{2}}$ as one-half spinors.

As a consequence of Eqs. (3) and (4), local densities and other observables can be represented as finite Fourier series in the angular variable θ so that the integrals over θ, needed in the calculation of various matrix elements, can be done analytically [16]. The remaining integrations (over the r and z variables) are performed by Gauss-Laguerre and Gauss-Hermite quadratures (with respectively 16 and twice

25 (for positive and negative z values) mesh points. The so-obtained real symmetric matrices are diagonalized using standard numerical methods.

In practice, the basis set must, of course, be truncated. It has been done upon using the deformation dependent prescription of Ref. [15],

$$\hbar\omega_\perp(n_\perp+1)+\hbar\omega_z\left(n_z+\tfrac{1}{2}\right)\leqslant\hbar\omega_0(N_0+2). \quad (5)$$

We have chosen $N_0=16$. It is a reasonable compromise between accuracy and feasibility to describe the whole fission barriers of actinide nuclei (see Ref. [18]). The usual axial harmonic oscillator parameters $b=\sqrt{m\omega_0/\hbar}$ and $q=\omega_\perp/\omega_z$, where m is the nucleon mass (which is approximated as being equal for neutron and proton, with $\hbar^2/2m=20.7355$ MeV fm^2), are determined by energy minimization.

The (b,q) parameters are fitted on a mesh of points separated by $\Delta\beta=0.01$ on the axial edges (prolate and oblate shapes) of the (β,γ) sextant.

Therefore, assuming that the basis parameters used for triaxial calculations should be close to those obtained in the axial calculation corresponding to the same β value, we have performed all triaxial calculations using the values of b and q retained in the axial cases by extrapolating them for a given value of β as a function of the scalar invariant $\cos(3\gamma)$. The HF + BCS equations are solved iteratively, as usual. The retained convergence criteria are 0.1 keV for the total energy and 0.01 barn for both $\widehat{Q}_{02}$ and $\widehat{Q}_{22}$ quadrupole moments.

B. Moments of inertia and adiabatic mass parameters

Out of the seven scalar functions of (β,γ) defining the Bohr Hamiltonian, the potential energy surface is obtained from the energy of the solutions yielded by the doubly constrained HF + BCS calculations. As already stated in the Introduction, the mass parameters for the rotational and vibrational modes (which constitute the six other functions) are evaluated upon using the Inglis-Belyaev formula (see Ref. [9]). This yields, for the moment of inertia associated with a rotation whose axis is perpendicular to the symmetry axis,

$$\mathcal{I}_\perp=\sum_{k,l}^{(1)}\frac{|\langle k|\hat{j}_+|l\rangle|^2}{E_k+E_l}(u_kv_l-u_lv_k)^2 + \frac{1}{2}\sum_{k,l}^{(2)}\frac{|\langle k|\hat{j}_+|\bar{l}\rangle|^2}{E_k+E_l}(u_kv_l-u_lv_k)^2 \quad (6)$$

where the first sum, labeled as (1), is performed on the members of all Kramers degenerate pairs of canonical basis states while the second sum, labeled as (2), is restricted to states such that $|K_l|=|K_k|=1/2$ (where K is the third component of the one-body angular momentum operator $\hat{j}_z$). The quantity v_i (u_i) is the usual BCS occupancy (inoccupancy) factor of the single-particle state i, and E_i represents the associated quasiparticle energy. This expression for the moment of inertia is, as is well known, an approximation of the ATDHFB approach in that it ignores the time-odd response of the solution to the time-odd self-consistent potential (see, e.g., Ref. [11]).

As for the vibrational mass parameter, we have made a further approximation for the adiabatic masses within the ATDFHB approach as discussed in Ref. [11] and dubbed there the $M(Q)$ mass approximation. This avoids the painful numerical derivation of normal and abnormal densities needed in the determination of the momentum operator $\hat{P}$ associated with the full adiabatic approach. It amounts to neglecting terms beyond the dynamical rearrangement, the static polarization effects produced upon changing the deformation. Hence, for the modes implying the operators $\hat{Q}_i$ and $\hat{Q}_j$, one writes the corresponding mass parameters as

$$B_{ij}=\hbar^2\frac{\mathcal{M}_{ij}^{(-3)}}{\mathcal{M}_{ij}^{(-1)^2}}, \quad (7)$$

where the moments $\mathcal{M}_{ij}^{(n)}$ are defined by

$$\mathcal{M}_{ij}^{(n)}=\sum_{k,l}^{(1)}(u_kv_l+u_lv_k)^2\langle k|\hat{Q}_i|l\rangle\langle l|\hat{Q}_j|k\rangle(E_k+E_l)^n. \quad (8)$$

Let us discuss now the approximation concerning the neglected dynamical polarization effect. In the rotational case, the corresponding correction can be evaluated by comparing such results with those of Routhian calculations [12]. It was found, within systematic Hartree-Fock-Bogoliubov calculations in Ref. [13], to yield an increase of the moment of inertia through a multiplicative factor of 1.32 on average. We have renormalized our moments of inertia accordingly.

In the vibrational case one does not enjoy such a straightforward point of comparison. This correction has been shown in the more simple Skyrme-Hartree-Fock case (where an exact approach can be somehow easily handled) for the axial quadrupole mode to depend on the nuclear matter effective mass associated with the considered effective interaction [10]. We have found, for an effective mass value in the expected 0.75 m range, that this mass parameter should be increased by about 20%. Yet, the effect of pairing correlations on this correction is unknown. This is why we have boldly taken here the same correction for vibrational mass parameters as the one used for moments of inertia.

From the above defined mass parameters associated with the collective modes parametrized by the expectation values of the operators $\widehat{Q}_{20}$ and $\widehat{Q}_{22}$ (noted with a transparent notation as B_{00}, B_{02}, and B_{22}), one gets readily those associated with the β and γ deformation parameters according to

$$B_{\beta\beta}=\frac{1}{D^2}[B_{00}\cos^2\gamma+2B_{02}\cos\gamma\sin\gamma+B_{22}\sin^2\gamma] \quad (9)$$

$$B_{\beta\gamma}=\frac{1}{D^2}[-B_{00}\cos\gamma\sin\gamma+B_{02}(\cos^2\gamma-\sin^2\gamma) + B_{22}\cos\gamma\sin\gamma] \quad (10)$$

$$B_{\gamma\gamma}=\frac{1}{D^2}[B_{00}\sin^2\gamma-2B_{02}\cos\gamma\sin\gamma+B_{22}\cos^2\gamma], \quad (11)$$

where D is defined, for a nucleus composed of A nucleons, by

$$D=\tfrac{3}{5}(r_0A^{1/3})^2, \quad (12)$$

using the usual radius parameter value $r_0=1.2$ fm.

C. Treatment of the Coulomb exchange contributions to the mean field and total energy

For the treatment of the exchange contribution of the Coulomb interaction to the total energy and, consequently, also to the mean field, the usual Slater approximation [19,20] has been used. It has been shown (see Refs. [21–23]) to be a very good approximation in absolute terms. Indeed, in the actinide region, for instance, it does not exceed 3% [23]. Yet, the error pattern shows a systematic trend correlated with the single-particle level density at the Fermi surface $\tilde{g}(\lambda)$. The absolute value of the error is larger for lower $\tilde{g}(\lambda)$ values.

This entails a systematic error on the fission barrier heights since $\tilde{g}(\lambda)$ values are always lower for the ground state than they are near the top of a fission barrier This effect was evaluated in Ref. [23] to lead to an underestimation of the inner barrier height by 310 keV in ^{238}U.

D. Choice of the intensity parameters of the seniority force

The intensities of the seniority residual interaction in use to describe $|T_z| = 1$ pairing correlations have been separately adjusted in the neutron-neutron and proton-proton cases. They are parametrized for the charge state q as

$$g_q = \langle k\bar{k}|\widehat{v}_{\text{residual}}|l\bar{l}\rangle = \frac{G_q}{11 + N_q}, \tag{13}$$

where $\widehat{v}$ is the antisymmetrized version of the two-body interaction $\widehat{v}$, N_q stands for the number of nucleons in the charge state q, and the set (l,k) labels any set of two single-particle states of the canonical basis.

To get realistic G_q values, we have calculated the following mass differences, e.g., for neutrons:

$$\Delta_n^{(3)}(N,Z) = \frac{(-1)^N}{2}[S_n(N,Z) - S_n(N+1,Z)], \tag{14}$$

where $S_n(N,Z)$ represents the neutron separation energy of a nucleus having N neutrons and Z protons. This expression could be easily modified to obtain the proton odd-even mass differences in isotonic nuclei. As noted in Refs. [24,25], these differences are mostly contingent upon pairing correlations for odd values of N or Z. Such a theoretical evaluation implies three microscopic calculations for the nuclei defined by the nucleon numbers $(N-1,Z)$, (N,Z), and $(N+1,Z)$. They have been performed for the relevant odd nuclei [26], within axially symmetric Hartree-Fock-BCS calculations, with self-consistent blocking, taking into account the genuine breaking of the time-reversal symmetry. Some care should be exercised in the choice of all the nuclei implied in such calculations. First they should be rigidly deformed, to avoid too large quantal shape fluctuations. They should also correspond to ground state solutions exhibiting robust pairing correlations, since the BCS approximation is known to be a poor representation of pairing properties in the low correlation regime. Finally, in odd-even or even-odd nuclei there is *a priori* an ambiguity in the solution to be considered in terms of the choice of quantum numbers. Here, these quantum numbers are the intrinsic parity and the third projection of the angular momentum K, which is well defined since our ground state solutions are axially symmetric. The quantum number K is assumed to represent the ground state angular momentum I within a Bohr-Mottelson unified model description (assuming the absence of Coriolis coupling). In Ref. [26] the authors retained the solutions corresponding to the experimental quantum numbers.

The resulting values of the G_q intensities depend of course on the effective interaction which is used to determine the mean field properties. In Ref. [26], the authors found the optimal set $G_n = G_p = -16$ MeV for the SkM* interaction in use here. This set yields a very satisfactory reproduction of the above discussed odd-even mass differences for the isotopes considered in this study. Indeed, the rms energy errors for the retained data are found to be 65 keV for neutrons and 130 keV for protons [26].

E. Approximate extraction of the spurious rotational energy content associated with the intrinsic wave function

It is well known that mean-field calculations corresponding to non-spherically-symmetric solutions yields a spurious rotational part in the corresponding total energy. This has been approximately corrected here, within a Lipkin ansatz [27]. It consists of assuming that the energy spectrum obtained by projecting the calculated intrinsic state on states having a good angular momentum I has the character of an exact rotor spectrum. This correction has been performed for axially symmetric solutions. In the vicinity of the inner barrier, in view of the relatively small value of the angle γ reached there, we have assumed that the corrective energies are the same as those obtained on the prolate edge of the (β,γ) sextant for the same value of β.

In the case considered here, namely of a zero angular momentum for the even-even fissioning nucleus (i.e., assuming again for our axially symmetric solutions that $K = I = 0$, à la Bohr-Mottelson ignoring any Coriolis coupling), one has

$$E_{I=0} = \langle\Psi|\widehat{H} - \frac{\hbar^2}{2\mathcal{I}}\widehat{\mathbf{J}}^2|\Psi\rangle, \tag{15}$$

where $|\Psi\rangle$ is the intrinsic wave function and $\widehat{\mathbf{J}}^2$ is the square of the total angular momentum operator. In the above, the moment of inertia $\mathcal{I}$ corresponds to a rotation around an axis perpendicular to the symmetry axis ($\mathcal{I}_\perp$) calculated within the Inglis-Belyaev ansatz plus a crude Thouless-Valatin correction, as above discussed.

As it turns out (see, e.g., [18]), upon increasing the deformation, the expectation value of the $\widehat{\mathbf{J}}^2$ operator increases more rapidly than the relevant moment of inertia. Consequently, this spurious rotational energy is found to be an increasing function of the elongation. In particular, it is thus larger at the top of the inner barrier than at the ground state. It thus lowers the fission barrier height from its intrinsic state value.

F. Solving the collective Bohr Hamiltonian Schrödinger equation

The five quadrupole collective coordinates α_μ, $\mu = -2, -1, \ldots, 2$ that describe the surface of a deformed nucleus, $R = R_0([\alpha_\nu])[1 + \sum_\mu \alpha_\mu Y^*_{2\mu}]$, are usually parametrized in terms of the two above defined (intrinsic) deformation parameters β

and γ, and three Euler angles $(\varphi,\theta,\psi) \equiv \Omega$ which define the orientation of the principal axes in the laboratory frame as

$$\alpha_\mu = \mathcal{D}^2_{\mu,0}(\Omega)\beta\cos\gamma + \frac{1}{\sqrt{2}}\left[\mathcal{D}^2_{\mu,2}(\Omega) + D^2_{\mu,-2}(\Omega)\right]\beta\sin\gamma, \tag{16}$$

where $\mathcal{D}^\lambda_{\mu\nu}$ is a usual Wigner function with the phase conventions of, e.g., Refs. [28,29].

The Hermitian Bohr Hamiltonian [14] describing the collective quadrupole dynamics, expressed in terms of the intrinsic variables, is given by

$$\widehat{H}_{\rm coll} = \widehat{T}_{\rm vib}(\beta,\gamma) + \widehat{T}_{\rm rot}(\beta,\gamma,\Omega) + V_{\rm coll}(\beta,\gamma). \tag{17}$$

The rotational kinetic energy may be written as

$$\widehat{T}_{\rm rot} = \frac{1}{2}\sum_{k=1}^{3}\frac{\widehat{J}_k^2}{\mathcal{I}_k}, \tag{18}$$

where $\mathcal{I}_k$ (with $k = 1,2,3$) are moments of inertia (for rotations along the k axis) and $\widehat{J}_k$ (with $k = 1,2,3$) intrinsic components of the total angular momentum operator.

The arbitrary quantization of the intrinsic kinetic energy operator acting on the collective wave functions is done as follows:

$$\begin{aligned}\widehat{T}_{\rm vib} = -\frac{\hbar^2}{2\sqrt{\omega b}}\Bigg\{&\frac{1}{\beta^4}\left[\frac{\partial}{\partial\beta}\left(\sqrt{\frac{b}{\omega}}\beta^4 B_{\gamma\gamma}\frac{\partial}{\partial\beta}\right) - \frac{\partial}{\partial\beta}\left(\sqrt{\frac{b}{\omega}}\beta^3 B_{\beta\gamma}\frac{\partial}{\partial\gamma}\right)\right]\\ &+\frac{1}{\beta\sin 3\gamma}\left[-\frac{\partial}{\partial\gamma}\left(\sqrt{\frac{b}{\omega}}\sin 3\gamma\, B_{\beta\gamma}\frac{\partial}{\partial\beta}\right) + \frac{1}{\beta}\frac{\partial}{\partial\gamma}\left(\sqrt{\frac{b}{\omega}}\sin 3\gamma\, B_{\beta\beta}\right)\frac{\partial}{\partial\gamma}\right]\Bigg\}.\end{aligned} \tag{19}$$

In the above, we have introduced two parameters ω and b, defined as

$$\omega = B_{\beta\beta}B_{\gamma\gamma} - B^2_{\beta\gamma}, \quad b = B_1B_2B_3 \tag{20}$$

The mass parameters (or vibrational inertial functions) $B_{\beta\beta}$, $B_{\beta\gamma}$, and $B_{\gamma\gamma}$ are, in general, functions of β and γ. The integration measure in the collective space is given by

$$d\tau_{\rm coll} = \beta^4|\sin 3\gamma|\sqrt{\omega b}\,d\beta\,d\gamma\,d\Omega. \tag{21}$$

The method used to solve the eigenvalue problem of the most general collective Hamiltonian (17) has been described in Refs. [29,30], where the eigenvalue problem is reduced to a simple matrix diagonalization, after having built an appropriate basis for each value of the angular momentum quantum number. For each value I of the angular momentum, one starts from a complete set of square integrable pairs of functions as

$$\phi^{IM}_{Kmn}(\beta,\gamma,\Omega) = \exp(-\mu^2\beta^2/2)\beta^n\begin{Bmatrix}\cos m\gamma\\ \sin m\gamma\end{Bmatrix}D^{I^*}_{MK}(\Omega). \tag{22}$$

For a given non-negative value of n, the allowed values of m are $m = n,n-2,\ldots,0$ or 1 (depending on the parity of n). The introduction of the Gaussian function $\exp(-\mu^2\beta^2/2)$ ensures that the basis states generate wave functions that vanish at large deformations ($\beta\to\infty$). The basis parameter μ has been adjusted for each nucleus individually, so that it yields a minimum of the ground state nuclear energy. The necessary symmetry conditions (see [28,31]) are fulfilled by restricting the space spanned by the states (22) upon using linear combinations of states

$$\xi^{IM}_{Lmn}(\beta,\gamma,\Omega) = e^{-\mu^2\beta^2/2}\beta^n\sum_{\text{even } K\geqslant 0} f^I_{LmK}(\gamma)\Phi^I_{MK}(\Omega) \tag{23}$$

which are invariant under the transformations of the octahedral group. The analytical form of the functions $f^I_{LmK}(\gamma)$ and the restrictions of the above summation on K values are discussed explicitly in Appendix A of Ref. [29]. The angular part corresponds to linear combinations of the Wigner functions

$$\Phi^I_{MK}(\Omega) = \sqrt{\frac{2I+1}{16\pi^2(1+\delta_{K0})}}\left[\mathcal{D}^{I^*}_{MK}(\Omega) + (-1)^I\mathcal{D}^{I^*}_{M-K}(\Omega)\right]. \tag{24}$$

In practice of course, such a basis has to be truncated. This has been done here by setting for n a maximum value $n_{\rm max} = 14$. The diagonalization of the collective Hamiltonian yields the energy spectrum E^I_α and the corresponding collective eigenfunctions

$$\Psi^{IM}_\alpha(\alpha,\beta,\Omega) = \sum_K \psi^I_{\alpha K}(\beta,\gamma)\Phi^I_{MK}(\Omega). \tag{25}$$

By using these collective wave functions, various observables (e.g., quadrupole E_2 reduced transition probabilities) can be calculated and compared with experimental results. For our purpose in this paper, we will restrict ourselves, however, to discussing merely the collective spectra associated with the quadrupole mode.

III. RESULTS AND DISCUSSION

A. Collective spectra in the ground state well

Calculations have been performed within the HF + BCS approach for the four considered actinide nuclei (^{236}U, ^{240}Pu, ^{248}Cm, and ^{252}Cf) on a regular mesh of 170 points covering the $(0,0.65)\times(0,60)$ sextant in the (β,γ) plane. The mesh sizes are equal to 0.05 (5) for the $\beta(\gamma)$ variables.

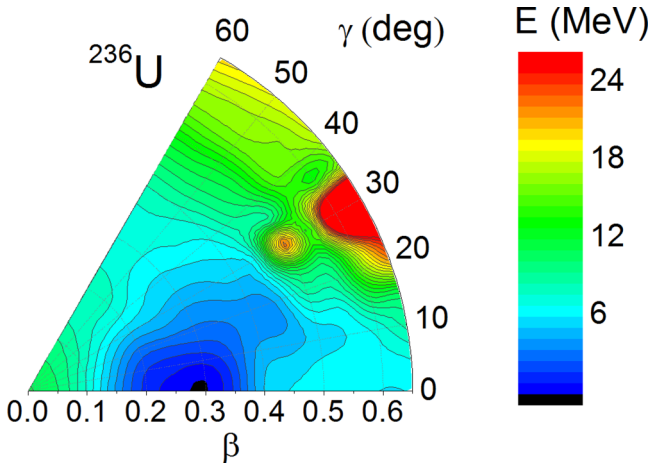

FIG. 1. Potential energy surface of the ^{236}U nucleus. The plotted energies are relative to the energy of the equilibrium point (indicated by the black dot) which is equal to −1778.23 MeV.

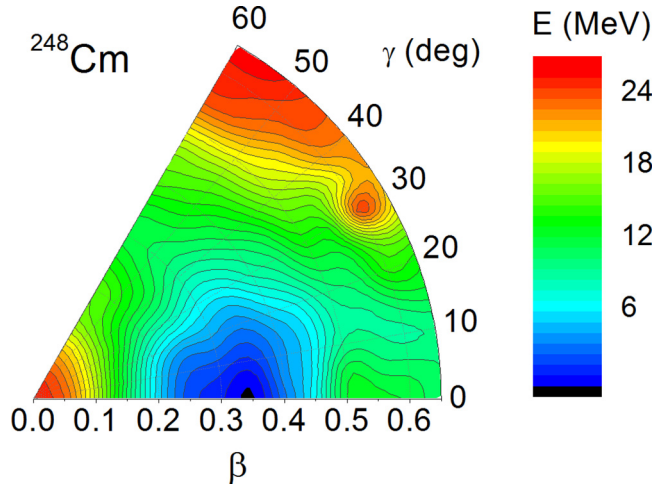

FIG. 3. Same as Fig. 1 for the ^{248}Cm nucleus. The energy of the equilibrium point is equal to −1848.52 MeV.

The seven scalar functions defining the Bohr collective Hamiltonian for the quadrupole modes have been determined as discussed above. The results obtained for the four PESs are displayed in Figs. 1–4. In all cases, the equilibrium solution (represented on the PES by a black dot) is located, as expected, on the prolate axis. The corresponding calculated deformations are quite consistent with the β deformation parameter values extracted from $B(E2)$ ground band data [32], as demonstrated in Table I.

Through the diagonalization of the Bohr Hamiltonian, we have obtained the low energy spectra of the four considered nuclei. Given the absence in the present calculations of any transition probability results, the energy levels are grouped arbitrarily, to some extent, mostly on the basis of standard patterns of well deformed nuclei in ground, β, and γ bands. Such calculated energy spectra are compared in Figs. 5–8 with experimental data [33–36] respectively.

As a general rule, the calculated ground band spectra are decompressed with respect to the data. This is due to two causes. First, the moments of inertia, calculated as discussed above, are too small. This yields, for instance, energies of the first 2^+ state which are too high (see Table II). The second reason for this global trend is related to the well-known Coriolis antipairing (CAP) effect [37]. It is clear that Routhian ATDHFB moments of inertia corresponding to low angular velocities Ω are less and less able, upon increasing Ω, to describe the quenching of the global rotational motion due to the pairing-induced counter-rotating intrinsic vortical motion.

As shown in Table II, both effects combine at an almost equal level to explain qualitatively the observed discrepancy, e.g., for the 12^+ energy level.

The effect of a bad reproduction of the rotational motion in the low angular velocity regime is evaluated for the 12^+ state through the following quantity (where the differentiation of the energy is performed around an energy averaged between

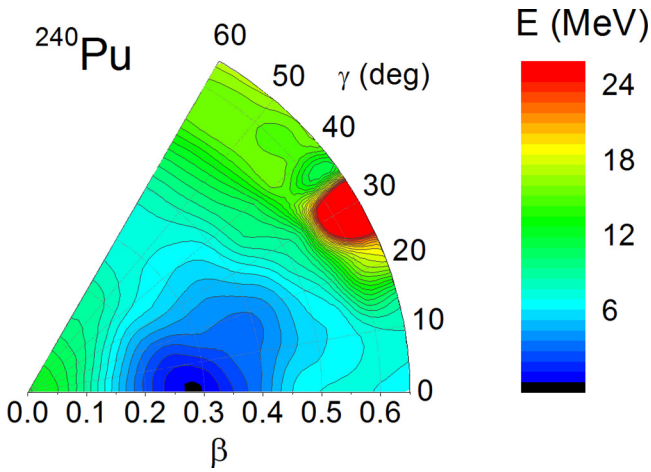

FIG. 2. Same as Fig. 1 for the ^{240}Pu nucleus. The energy of the equilibrium point is equal to −1800.40 MeV.

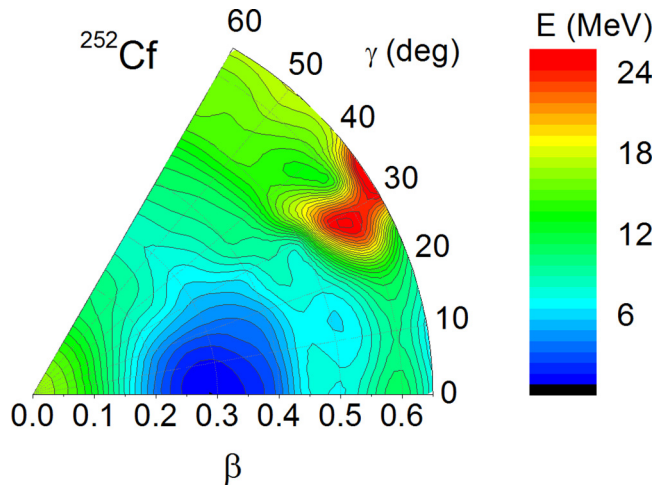

FIG. 4. Same as Fig. 1 for the ^{252}Cf nucleus. The energy of the equilibrium point is equal to −1867.30 MeV.

TABLE I. Experimental (calculated) values of the β deformation parameter noted "Exp." (noted "Calc.") at equilibrium deformation. Experimental data are taken from [32].

Nuclei	^{236}U	^{240}Pu	^{248}Cm	^{252}Cf
Exp.	0.282	0.289	0.297	0.304
Calc.	0.272	0.294	0.301	0.294

the experimental and calculated values):

$$\Delta E_{\mathrm{low}\,\Omega} = \frac{E_{\mathrm{exp}}(12^+) + E_{\mathrm{calc}}(12^+)}{E_{\mathrm{exp}}(2^+) + E_{\mathrm{calc}}(2^+)}[E_{\mathrm{calc}}(2^+) - E_{\mathrm{exp}}(2^+)], \tag{26}$$

whereas the corresponding CAP energy correction is determined as

$$\Delta E_{\mathrm{CAP}} = 78\hbar^2\left[\frac{1}{\mathcal{I}_{\mathrm{exp}}(2^+)} - \frac{1}{\mathcal{I}_{\mathrm{exp}}(12^+)}\right], \tag{27}$$

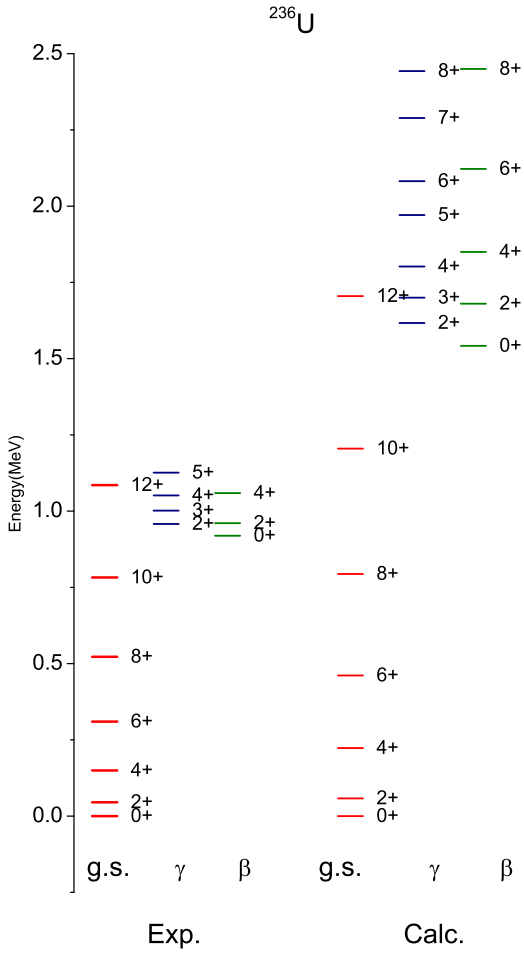

FIG. 5. Experimental (Exp.) [33] and calculated (Calc.) low energy spectra in ^{236}U.

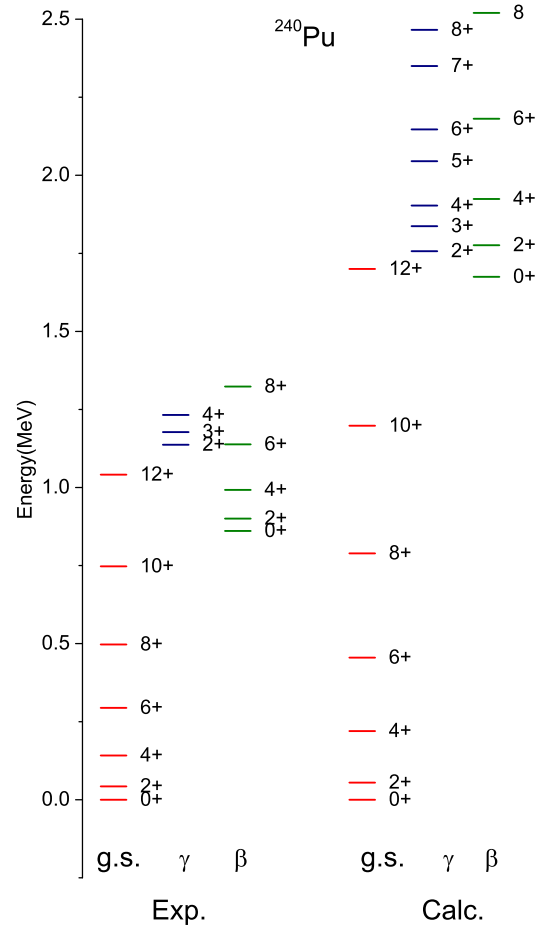

FIG. 6. Same as Fig. 5 for ^{240}Pu. The experimental spectrum is taken from Ref. [34].

where the experimental moment of inertia is defined as usual as

$$\mathcal{I} = \frac{4\hbar^2}{E_{\mathrm{exp}}(I-2) - 2E_{\mathrm{exp}}(I) + E_{\mathrm{exp}}(I+2)}. \tag{28}$$

Note that the attribution to the CAP effect only—of all the experimentally observed variations of the moments of inertia—is fully justified, for these nuclei in this angular velocity range, by the pairing-induced intrinsic vortical mode calculations of Refs. [38,39].

Regarding the β and γ vibrational modes, one may propose, at least qualitatively, the following explanation for part of their too high calculated phonon energies, beyond possible bad pairing force intensities. Note *en passant* that this is a usual feature of similar calculations (see, e.g., [40–42]). Indeed, in the considered one-phonon states, one should observe a pairing quenching due to the Pauli blocking of pair transfers on orbits partially filled by particle-hole excitations generating the vibrational correlations.

Yet it is particularly significant that, in all considered cases, the calculated relative order of β and γ band heads is consistent with the data (β band heads lower than γ ones for ^{236}U and ^{240}Pu and conversely for ^{248}Cm).

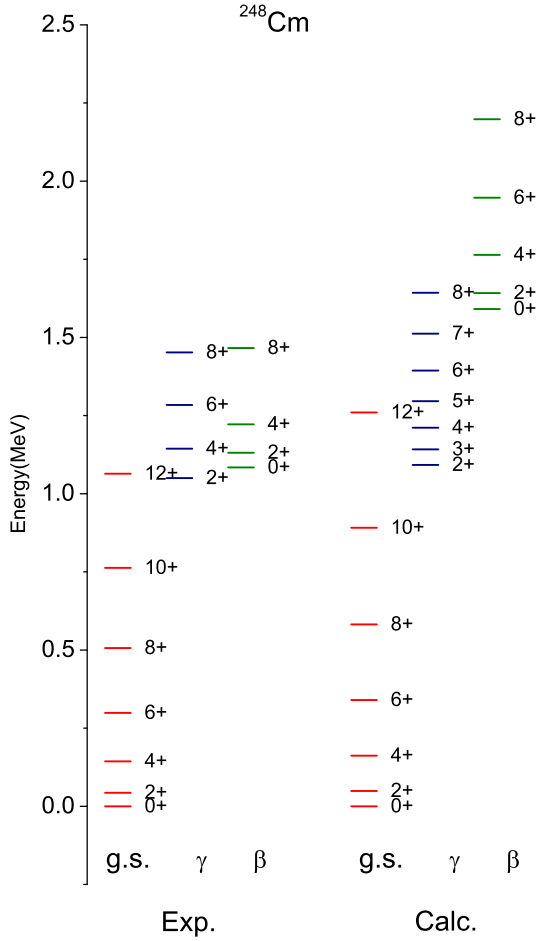

FIG. 7. Same as Fig. 5 for ^{248}Cm. The experimental spectrum is taken from Ref. [35].

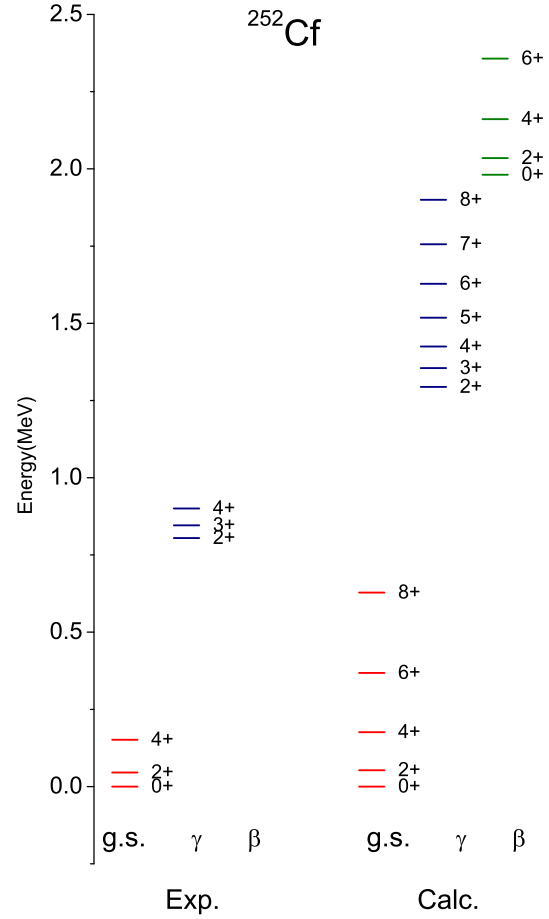

FIG. 8. Same as Fig. 5 for ^{252}Cf. The experimental spectrum is taken from Ref. [36].

It is interesting to compare in detail our results with those of Ref. [42]. There, the calculations have been performed within the same approach as ours (up to minor details: our angular mesh size is slightly smaller—5 degrees instead of 6—and our estimate of the so-called Thouless-Valatin correction differs by 0.02) and up to one isotope (^{236}U) our calculated nuclei have also been calculated there. The main difference lies in the intensity of the pairing interaction in use. In our case it has been fitted, as already mentioned, by performing explicitly what is generally claimed to be done; namely, by a fit to odd-even mass differences (not through some minimal quasiparticle approximate consideration but by just getting, as one should, odd-even mass differences from consistently calculated solutions). As a result, our residual interaction appears to be significantly more intense than in the considered paper. This is clearly visible from the too high inner fission barrier which the other paper displays (it is obtained to be about 12 MeV in ^{242}Pu for an axially symmetric solution without rotational correction using the same SkM* interaction).

A large part of the discrepancies between data and our results for the spectra are inherent, as above discussed, to the Bohr Hamiltonian approach. This clearly prevents drawing conclusions beyond qualitative statements from such calculations. Another part of the loose description of the energy levels is due to a description of pairing correlations at low Ω regimes which is not accurate enough. This may result from various causes: a poor analytical form for the residual interaction in use, an inaccurate determination of its intensity parameters, the crude handling of Thouless-Valatin corrective terms, the BCS (or HFB) approximation itself–in particular in

TABLE II. Experimental energies $E_{\rm exp}(2^+)$ and $E_{\rm exp}(12^+)$ of the 2^+ and 12^+ states of the ground band in comparison with their calculated counterparts $E_{\rm calc}(2^+)$ and $E_{\rm calc}(12^+)$. The corrective energies $\Delta E_{\rm low\,\Omega}$ for the 12^+ states due to our bad reproduction of low-Ω rotational properties are also displayed together with the correction energy $\Delta E_{\rm CAP}$ for these states due to the neglect of the CAP effect in Bohr Hamiltonian calculations. The energies $\Delta E_{\rm low\,\Omega}$ and $\Delta E_{\rm CAP}$ are defined in the text. All energies are expressed in keV. Note the absence of data concerning the 12^+ state for the ^{252}Cf nucleus.

Nucleus	$E_{\rm exp}(2^+)$	$E_{\rm calc}(2^+)$	$E_{\rm exp}(12^+)$	$E_{\rm calc}(12^+)$	$\Delta E_{\rm low\,\Omega}$	$\Delta E_{\rm CAP}$
^{236}U	45	58	1085	1704	352	429
^{240}Pu	43	55	1041	1700	336	312
^{248}Cm	43	49	1064	1260	177	332
^{252}Cf	46	53		1357		

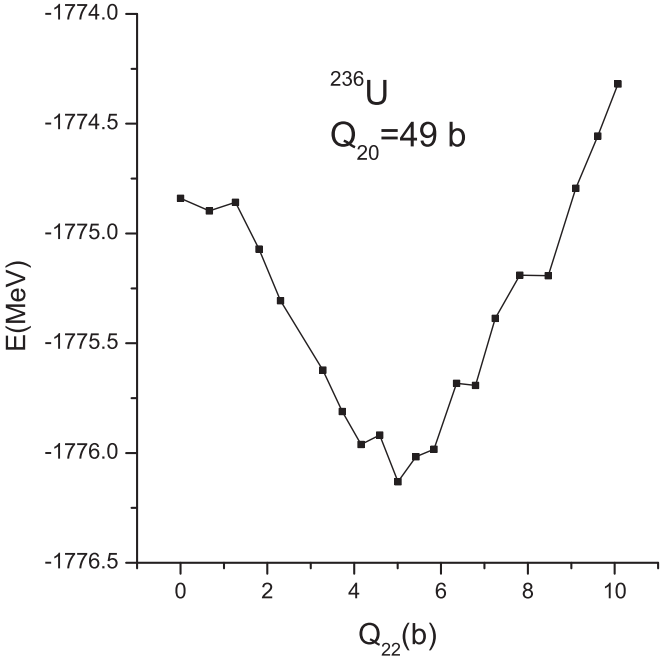

FIG. 9. Section of the potential energy surface of ^{236}U as a function of Q_{22} (in barns), for a given value of Q_{20} (in barns), in the inner saddle point region. Energies are given in MeV.

its inherent nonconservation of the particle numbers—or the purely static character of our pairing treatment. Regarding the last point, it is our contention that, while it is *a priori* better to enlarge the space of collective variables, a fair assessment of the importance of doing so requires first that the other points be carefully considered.

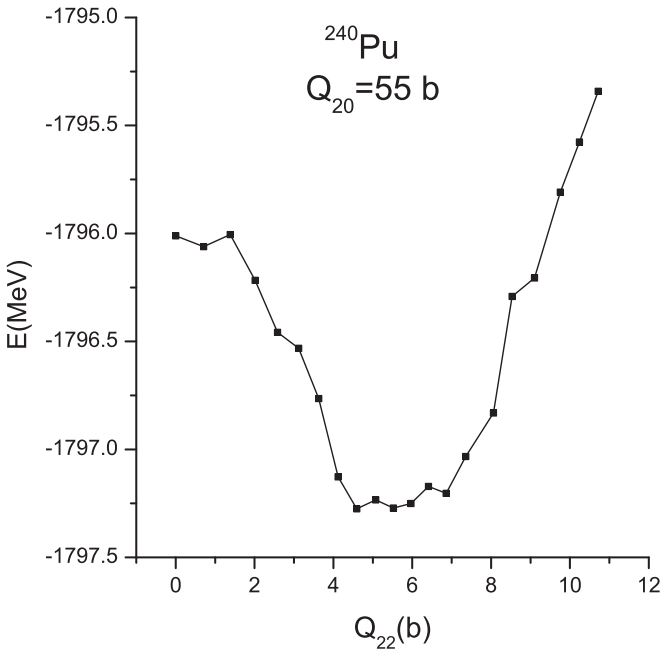

FIG. 10. Same as Fig. 9 for ^{240}Pu.

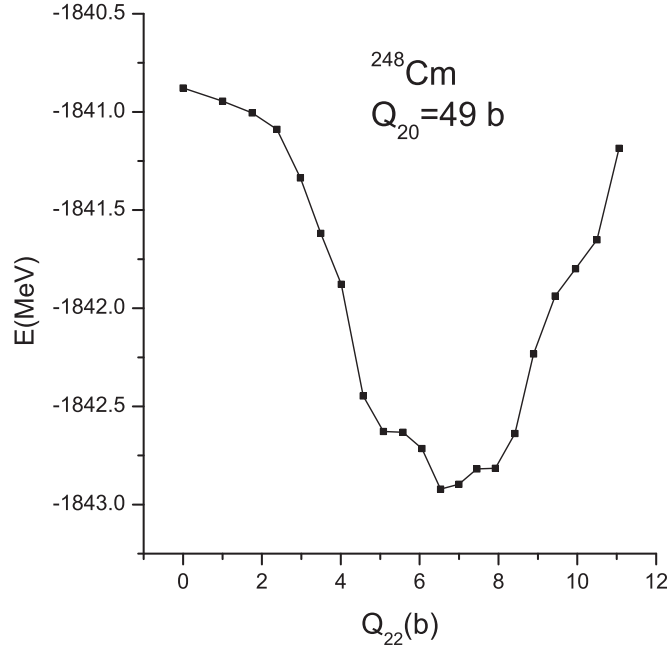

FIG. 11. Same as Fig. 9 for ^{248}Cm.

B. Potential energy landscape around the inner barrier

As already discussed, various static calculations of PESs in heavy nuclei (see, e.g., [1,18,43]) have demonstrated the existence of a triaxial instability in the vicinity of the inner barrier. As a consequence, the total nuclear energy is lowered at the first saddle point when allowing triaxial shapes for the nucleus undergoing fission. This is illustrated on Figs. 9–12 where, Q_{20} being fixed at its value obtained for the axial saddle point, we display the total energy as a function of Q_{22}.

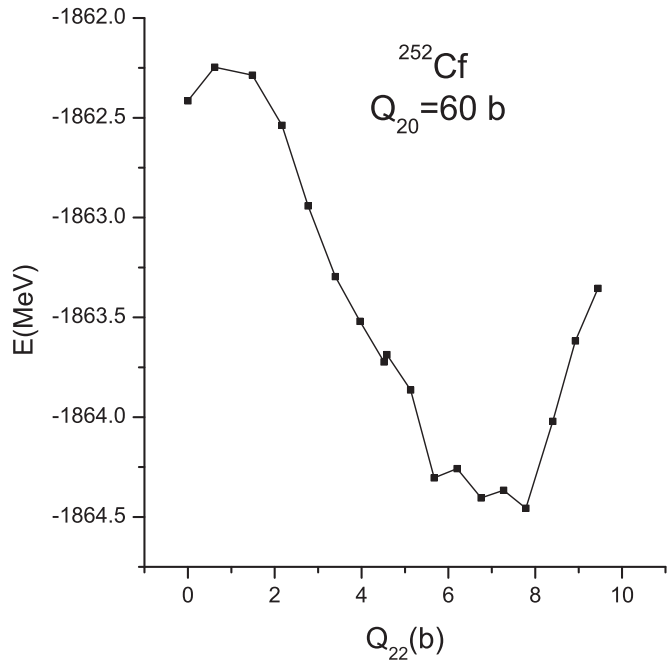

FIG. 12. Same as Fig. 9 for ^{252}Cf.

TABLE III. Deformation parameter β values corresponding to the axial inner barrier solution ($\beta_{\rm IB}^{\rm axial}$) together with the corresponding triaxial values $\beta_{\rm IB}^{\rm triax}$ along with the associated γ values ($\gamma_{\rm IB}^{\rm triax}$).

Nuclei	^{236}U	^{240}Pu	^{248}Cm	^{252}Cf
$\beta_{\rm IB}^{\rm axial}$	0.510	0.562	0.547	0.567
$\beta_{\rm IB}^{\rm triax}$	0.526	0.560	0.540	0.580
$\gamma_{\rm IB}^{\rm triax}$	10.9	10.1	11.9	12.3

Of course, the value of the axial quadrupole deformation parameter β may vary between what one obtains for the axial inner barrier solution and the triaxial one. However, these differences are small as demonstrated in Table III. The γ values corresponding to the triaxial saddle point are found in the 10–12 range, as seen also in Table III.

Upon releasing the axial symmetry one lowers the inner saddle point energy by a quantity $\Delta E_{\rm IB}^{\rm triax}$ defined, with an obvious notation, as

$$\Delta E_{\rm IB}^{\rm triax} = E\left(\beta_{\rm IB}^{\rm triax.},\gamma_{\rm IB}^{\rm triax.}\right) - E\left(\beta_{\rm IB}^{\rm axial},0\right) \qquad (29)$$

As seen in Table IV and already noticed (see, e.g., [18]), this energy correction is an increasing function of the nucleon number A: from 1.14 MeV for ^{236}U to 2.47 for ^{252}Cf.

C. Inner barrier heights

Starting from the results of axially symmetric HF + BCS calculations, we evaluate the inner barrier heights by adding various corrections.

First, we have assumed that for all the considered nuclei the basis size is sufficient to obtain the convergence of the energy difference between the ground state and the axial inner barrier solutions. This takes stock of the results of [18] for the ^{252}Cf nucleus obtained with the same Skyrme force and almost the same seniority force parametrization (see Table I in Ref. [18]).

As discussed in Sec. II C, the use of the Slater approximation for the treatment of the Coulomb exchange contribution to the total energy and the Hartree-Fock mean field yields an underestimation of the inner barrier. It is found to be given by $\Delta E^{\rm Slater} = 310$ keV in the ^{238}U nucleus [23]. Owing to the systematic character of such an underestimation, as discussed in Ref. [23], and to the numerically heavy character of such exact Coulomb exchange calculations, we have simply assumed here that it takes the same value for the four nuclei under study.

TABLE V. Rotational energies (in MeV) at the ground state deformation ($E_{GS}^{\rm rot}$) and at the axial saddle point ($E_{\rm IB}^{\rm rot}$) along with the deduced rotational energy correction to the axial inner barrier ($\Delta E^{\rm rot}$).

Nucleus	$E_{GS}^{\rm rot}$	$E_{\rm IB}^{\rm rot}$	$\Delta E^{\rm rot}$
^{236}U	1.67	2.31	−0.64
^{240}Pu	1.57	2.42	−0.85
^{248}Cm	1.81	2.24	−0.43
^{252}Cf	1.68	2.22	−0.54

The spurious rotational energy correction $\Delta E^{\rm rot}$ for an even-even fissioning nucleus with $I^+ = 0^+$ has been evaluated *à la* Lipkin as discussed in Sec. II E [see Eq. (15)]. As seen in Table V, it lowers the inner barrier height by about half a MeV.

As shown in Table IV, by adding these corrections one obtains inner barrier heights $E_{\rm IB}^{\rm axial}$ which are significantly too high with respect to experimental estimates when axial symmetry is imposed. This leaves room for a decrease due to the release of the axial symmetry constraint as discussed now.

Finally, we add to these $E_{\rm IB}^{\rm axial}$ energies the gain in energy $\Delta E^{\rm triax}$ obtained when considering the triaxial saddle point for the inner barrier. The resulting inner barrier heights $E_{\rm IB}^{\rm calc}$ compare reasonably well with the recommended values deduced from experimental data of Ref. [44] for the two lightest nuclei calculated nuclei (^{236}U, ^{240}Pu). The calculated barrier heights of the two other considered nuclei (^{248}Pu, ^{252}Cf) are too high by about 1 MeV.

In a previous similar study [18] using the same SkM* Skyrme parametrization, the authors had considered intensities of the residual interaction which were significantly lower than what is in use here. Expectedly, the calculated heights of the inner fission barrier were considerably overestimated. Making appropriate comparisons—namely neglecting in our case the correction due to the Slater approximation—their inner barrier heights (for triaxial solutions with rotational correction) are found to be higher than ours by about 1.3 MeV in the ^{236}U, ^{240}Pu, and ^{252}Cf nuclei where the comparison can be made.

TABLE IV. Inner fission barrier heights and associated corrective terms (in MeV) for the ^{236}U, ^{240}Pu, ^{248}Cm, and ^{252}Cf nuclei. The following quantities are listed: axially symmetric HF + BCS inner barrier heights $E_{\rm IB}^{\rm axial}$(uncorr.), rotational energy corrections $\Delta E^{\rm rot}$, Coulomb exchange corrections $\Delta E^{\rm Slater}$ (MeV), inner barrier heights corrected for the spurious rotational energy content, assuming axial symmetry $E_{\rm IB}^{\rm axial}$(corr.), energy corrections due to the triaxiality of the solutions $\Delta E^{\rm triax}$, resulting calculated inner barrier heights $E_{\rm IB}^{\rm calc}$, and finally $E_{\rm IB}^{\rm exp}$, the estimated inner barrier heights from experimental data taken from Ref. [44].

Nucleus	$E_{\rm IB}^{\rm axial}$(uncorr.)	$\Delta E^{\rm rot}$	$\Delta E^{\rm Slater}$	$E_{\rm IB}^{\rm axial}$(corr.)	$\Delta E^{\rm triax}$	$E_{\rm IB}^{\rm calc}$	$E_{\rm IB}^{\rm exp}$
^{236}U	6.77	−0.64	0.31	6.44	−1.14	5.30	5.0(3)
^{240}Pu	8.02	−0.85	0.31	7.48	−1.43	6.05	5.8(3)
^{248}Cm	9.21	−0.43	0.31	9.09	−2.27	6.82	5.9(3)
^{252}Cf	8.82	−0.54	0.31	8.59	−2.47	6.12	5.3(3)

IV. CONCLUSIONS

Our HF+BCS microscopic approach of the collective dynamics (corresponding to the usual β and γ degrees of freedom) yields low energy spectra which reproduce qualitatively the data for the four considered nuclei. However, our results are of slightly lesser quality than those of Ref. [42] due to too small adiabatic mass parameters and moments of inertia. On the other hand, the more intense residual interaction that we used allowed us to yield calculated heights of the inner fission barrier in excellent agreement (given the uncertainties of the so-called experimental estimates) for the ^{236}U and ^{236}Pu nuclei and only too high by 1 MeV for the ^{248}Cm and ^{252}Cf nuclei. This does not seem to be the case for the calculations of Ref. [42] (as inferred from the scarce information given in the paper on fission barriers) as well as of those reported in another previous study [18] due to too weak pairing correlations.

This apparent contradiction between the quality in reproducing collective spectroscopy and fission properties may point in the direction of some deficiencies of either the theoretical framework or the way in which it is implemented, or both. This is why even though our approach yields results which are encouraging, some improvements are called for. While some care has been exerted to determine parameters of the seniority force yielding reasonable odd-even mass differences in the actinide region, a better treatment of pairing correlations is still to be made. This concerns, in particular, the particle number conservation. To improve on this point, similar calculations using the so-called highly truncated diagonalization approach (HTDA) [45] are currently being performed along the lines of the work presented in Ref. [46], for nuclei in the $A = 100$ region.

Upon using a better static description of pairing correlations and the resulting determination of the least action trajectories, we will be able to provide better grounds for the evaluation of fission half-lives. It will be interesting, in particular, to assess whether or not the consideration of an explicit dynamical account of pairing correlations is at all required in this respect.

ACKNOWLEDGMENTS

One of us (P.Q.) thanks the Laboratoire N-Corps et Structure de la Matière of the Algiers Ecole Normale Supérieure, and another (D.E.M.) thanks the Centre d'Etudes Nucléaires de Bordeaux-Gradignan for the warm hospitality extended during several visits. Illuminating discussions with L. Bonneau are also gratefully acknowledged. We thank also M. Rebhaoui for his help in the completion of the manuscript.

[1] V. V. Pashkevich, Nucl. Phys. A **133**, 400 (1969).
[2] R. A. Gherghescu, J. Skalski, Z. Patyk, and A. Sobiczewski, Nucl. Phys. A **651**, 237 (1999).
[3] J. Sadhukhan, J. Dobaczewski, W. Nazarewicz, J. A. Sheikh, and A. Baran, Phys. Rev. C **90**, 061304(R) (2014).
[4] J. Zhao, B.-N. Lu, T. Nikšić, D. Vretenar, and S.-G. Zhou, Phys. Rev. C **93**, 044315 (2016).
[5] J. Bartel, P. Quentin, M. Brack, C. Guet, and H.-B. Håkansson, Nucl. Phys. A **386**, 79 (1974).
[6] H. Krivine, J. Treiner, and O. Bohigas, Nucl. Phys. A **336**, 155 (1980).
[7] M. H. Koh, L. Bonneau, P. Quentin, T. V. Nhan Hao, and H. Wagiran, Phys. Rev. C **95**, 014315 (2017).
[8] Chart of Nuclides, National Nuclear Data Center, Brookhaven National Laboratory, 2017, http://www.nndc.bnl.gov/chart/.
[9] S. T. Belyaev, Nucl. Phys. A **24**, 322 (1961), and references quoted therein.
[10] M. J. Giannoni and P. Quentin, Phys. Rev. C **21**, 2060 (1980); **21**, 2076 (1980).
[11] E. Kh. Yuldashbaeva, J. Libert, P. Quentin, and M. Girod, Phys. Lett. B **461**, 1 (1999).
[12] D. J. Thouless and J. G. Valatin, Nucl. Phys. **31**, 211 (1962).
[13] J. Libert, M. Girod, and J. P. Delaroche, Phys. Rev. C **60**, 054301 (1999).
[14] Å. Bohr, K. Dan. Vidensk. Selsk. Mat. Fys. Medd. **26**, 1 (1952).
[15] H. Flocard, P. Quentin, A. K. Kerman, and D. Vautherin, Nucl. Phys. A **203**, 433 (1973).
[16] D. Samsoen, P. Quentin, and J. Bartel, Nucl. Phys. A **652**, 34 (1999).
[17] D. Vautherin, Phys. Rev. C **7**, 296 (1973).
[18] L. Bonneau, P. Quentin, and D. Samsoen, Eur. Phys. J. A **21**, 391 (2004).
[19] C. von Weiszæcker, Z. Phys. **96**, 431 (1936).
[20] C. Slater, Phys. Rev. **81**, 385 (1951).
[21] C. Titin-Schnaider and P. Quentin, Phys. Lett. B **49**, 397 (1974).
[22] J. Skalski, Phys. Rev. C **63**, 024312 (2001).
[23] J. Le Bloas, M.-H. Koh, P. Quentin, L. Bonneau, and J. I. A. Ithnin, Phys. Rev. C **84**, 014310 (2011).
[24] J. Dobaczewski, P. Magierski, W. Nazarewicz, W. Satuła, and Z. Szymanski, Phys. Rev. C **63**, 024308 (2001).
[25] T. Duguet, P. Bonche, P.-H. Heenen, and J. Meyer, Phys. Rev. C **65**, 014310 (2001).
[26] M.-H. Koh, D. D. Duc, T. V. Nhan Hao, H. T. Long, P. Quentin, and L. Bonneau, Eur. Phys. J. A **52**, 3 (2016).
[27] H. J. Lipkin, Ann. Phys. (NY) **9**, 272 (1960).
[28] D. A. Varshalovich, A. N. Moskalev, and V. K. Khersonskii, *Quantum Theory of Angular Momentum* (World Scientific, Singapore, 1988).
[29] L. Próchniak, K. Zajac, K. Pomorski, S. G. Rohoziński, and J. Srebrny, Nucl. Phys. A **648**, 181 (1999).
[30] G. G. Dussel and D. R. Bes, Nucl. Phys. A **143**, 623 (1970).
[31] K. Kumar and M. Baranger, Nucl. Phys. A **92**, 608 (1967).
[32] S. Raman, C. W. Nestor, Jr., and P. Tikkanen, At. Data Nucl. Data Tables **78**, 1 (2001).
[33] E. Browne and J. K. Tuli, Nucl. Data Sheets **107**, 2649 (2006).
[34] B. Singh and E. Browne, Nucl. Data Sheets **109**, 2439 (2008).
[35] M. J. Martin, Nucl. Data Sheets **122**, 377 (2014).
[36] N. Nica, Nucl. Data Sheets **106**, 813 (2005).
[37] B. R. Mottelson and J. G. Valatin, Phys. Rev. Lett. **5**, 511 (1960).

[38] B. Nerlo-Pomorska, K. Pomorski, P. Quentin, and J. Bartel, Phys. Scr. **89**, 054004 (2014).
[39] P. Quentin and J. Bartel (unpublished).
[40] L. Próchniak, P. Quentin, D. Samsoen, and J. Libert, Nucl. Phys. A **730**, 59 (2004).
[41] J. P. Delaroche, M. Girod, J. Libert, H. Goutte, S. Hilaire, S. Peru, N. Pillet, and G. F. Bertsch, Phys. Rev. C **81**, 014303 (2010).
[42] L. Próchniak, Int. J. Mod. Phys. E **17**, 160 (2008).
[43] P. Möller and J. R. Nix, in *Proceedings of the IAEA Symposium on Physics and Chemistry of Fission, Rochester, 1973*, Vol. I (IAEA, Vienna, 1974), p. 103.
[44] G. N. Smirenkin, IAEA Technical Report No. INDC(CCP)-359 (unpublished).
[45] N. Pillet, P. Quentin, and J. Libert, Nucl. Phys. A **697**, 141 (2002).
[46] M. Imadalou, D. E. Medjadi, P. Quentin, and L. Próchniak, Eur. Phys. J. **89**, 054025 (2014).